



ISSN: 0975-833X

RESEARCH ARTICLE

EVALUATING THE INHIBITING ACTION OF CdS NANOPARTICLES AND CdS/PMMA HYBRID FOR CORROSION OF CARBON STEEL IN ACIDIC MEDIA

*Ibrahim M. Nassar, Mohamed A. Abbas, A. Hamdy and Olfat. E. El-azabawy

Egyptian Petroleum Research Institute (EPRI), 1 Ahmed El-Zomor St., Nasr City, 11727, Cairo, Egypt

ARTICLE INFO

Article History:

Received 25th September, 2013
Received in revised form
22nd September, 2013
Accepted 20th October, 2013
Published online 31st December, 2013

Key words:

Carbon steel, Corrosion,
Acid inhibition, Polarization, EIS.

Copyright © Ibrahim M. Nassar, et al. This is an open access article distributed under the Creative Commons Attribution License, which permits unrestricted use, distribution, and reproduction in any medium, provided the original work is properly cited.

ABSTRACT

Corrosion inhibition of C-steel in HCl solution using CdS and CdS/Polymethylmethacrylate hybrid has studied by weight loss, Tafel polarization and electrochemical impedance spectroscopy. The results show that CdS acted as a good inhibitor and this inhibition efficiency enhanced by using CdS/PMMA hybrid. This inhibitory action increases with increasing the inhibitor concentration but decreases with rising the temperature. Polarization curves indicated that both CdS and CdS/PMMA acted as mixed inhibitor. Thermodynamic study revealed that the adsorption of CdS and CdS/PMMA obeys the Langmuir isotherm. The inhibition effect of the investigated inhibitors confirmed by EDX and XRD techniques.

INTRODUCTION

Nowadays, steel has become an important part of our life due to its extensively applications in automotive, household appliances, business machine and heavy construction such as marine and chemical industries (Bardel 2003). Even with advanced corrosion resistant materials available, carbon steel has been widely employed as construction materials for pipe in the oil and gas production as well as down hole tubular, flow lines and transmission pipelines (Hegazy *et al.*, 2013; Ridd *et al.*, 1998). In oil fields, hydrochloric acid solution recommended as the cheapest way to dissolve calcium carbonate scale inside the pipelines under most conditions. Accordingly, corrosion inhibitors injected with the hydrochloric acid solution to avoid the destructive effect of acid on the surface of the pipelines (Oddo and Tomson 1982). It generally assumed that the corrosion inhibition performed by chemical compounds added to the electrolyte is attributed, almost as a first stage, to the adsorption of additives (ions or neutral polar molecules) to the metal/solution interface (Popova *et al.*, 2004). Inorganic particles have steadily grown because of the great expectations for their application in different fields of material science and technology. This is due to their unique properties: catalytic, optical, semiconductive, magnetic, antifriction and others. Most of unique and advanced properties are inherent to bare nanoparticles of metals and semiconductor compounds. However, bare nanoparticles usually possess excessive surface energy and should be protected (surface capping or modification) or placed in an inert matrix for use in most applications (Zheludkevich *et al.*, 2005). Influence of inorganic components on hybrid

nanocomposite is: (1) increasing adhesion between metals and hybrid coatings; (2) used as adhesion promoters for pre-treatments of metals; (3) improving comprehensive performances of polymer in hybrid coatings. Typical advantages of traditional polymer coatings systems are they are mechanically flexible and tough, but have poor abrasion and thermal resistance. Inorganic sols provide a good adhesion layer between metallic substrate and organic coatings, which related to the low oxygen diffusion and the good mechanical properties (Brinker and Scherer 1990). PMMA- Silica hybrid coating found to be greatly improving corrosion resistance of stainless steel (Varela Caselis *et al.*, 2012). When sol-gel hybrid coatings are applied, strong van der Waals bonds between films and metal surface formed at first and transformed to stable covalent bonds during drying stage of the films. The sintering activity usually increases with decreasing particle size (Liu *et al.*, 1998). Owing to the increasing surface per weight ratio of nanoparticles, their surface dependent reactions become kinetically more and more important. Therefore, bodies made of nanoparticles density and combine to firm compounds at rather low temperatures. This allows using them for the production of glass-like inorganic coatings by a thermal process even suitable for the application on light metals (Nguyen *et al.*, 2002). Appropriate additives, forming eutectic mixtures with silicon dioxide, e.g. boron oxide or phosphorous oxide, may lower the necessary sintering temperature even further and increase the chemical stability of the coatings. The aim of the present paper is to investigate the corrosion protective capability of the prepared inorganic-organic hybrid material by electrochemical corrosion tests, as well as studying the effect of CdS nanoparticles on the corrosion efficiency of the polymer.

*Corresponding author: Ibrahim M. Nassar, email: inassar32@yahoo.com.
Tel: +2(02)22745902, Fax +2(02)227727433. City, 11727, Cairo, Egypt

MATERIALS AND METHODS

The weight losses as well as electrochemical studies performed on carbon steel strips having a composition (wt. %): C 0.14, Mn 0.035, Si 0.17, S 0.025, P 0.03 and balance Fe. Aggressive solution of hydrochloric acid (AR grade) used for all studies and double distilled water is used to prepare the acid solutions.

Inhibitors

Preparation of CdS nanoparticles

CdS with thiophenol capping were synthesized as following: 0.1M cadmium salt solution (Cd^{2+}) was prepared by dissolving cadmium nitrate in methanol then another solution of 0.1 M, Na_2S (S^{2-}) was prepared by dissolving 80gm of sodium sulphide in 50ml of methanol and 0.2M thiophenol solution was made by mixing 2.2ml of thiophenol with 100ml of methanol. Then, 50ml of sodium sulphide solution mixed with 50 ml of thiophenol solution and stirred; finally, a 100ml of cadmium nitrate added to the solution accompanied with stirring. This yields a cloudy yellow solution, and then the solution stirred for some more time, filtered and suction dried (Shikha and Sanjay 2006).

Preparation of CdS/PMMA nanocomposite

For the preparation of CdS-PMMA composite, PMMA of laboratory grade dissolved in Tetra hydrofurane (THF) solvent and 10 % of PMMA chalcogenide CdS nanoparticles dispersed in this PMMA solution. This solution was then stirred using magnetic stirrer and then poured into flat- bottomed petri dishes to form film with a thickness of ~ 0.05 mm. The solvent allowed evaporating slowly over a period of 24 hours in dry atmosphere. The obtained film was then peeled off and dried in a vacuum at 50°C , well below the boiling point of solvent to avoid bubbling, for 24 hours in order to ensure the removal of the solvent (Favier *et al.*, 1997; Chazeau *et al.*, 1999).

Weight loss measurements

The weight loss study carried on carbon steel specimens of $5.0 \times 2.0 \times 0.025$ cm. The working specimens polished with different grades of emery papers, degreased in acetone, washed with bi- distilled water and finally dried. The weight loss study conducted in the temperature range 298-333 K.

Electrochemical measurements

The electrochemical studies carried out using a three-electrode cell assembly at room temperature. The working electrode was a carbon steel of 1 cm^2 area and the rest being covered by using commercially available lacquer. A Platinum wire used as counter electrode and saturated calomel electrode (SCE) as reference electrode. The polarization and impedance studies carried out using a Radiometer Voltalab master (Model PGZ 301) with EIS software program Zsimpwin. For polarization measurements the potential was swapped from -800 to -300 mV with respect to OCP at a sweep rate 2 mVs^{-1} . The linear Tafel segment of anodic and cathodic curves were extrapolated to corrosion potential to obtain the corrosion current densities (I_{corr}). The impedance studies were carried out using ac signals of 10 mV amplitude for the frequency spectrum from

100 kHz to 50 mHz after 30 min of immersion time to stabilize the system. The value of charge transfer resistance obtained from the diameter of the semi circles of the Nyquist plots.

Surface Film Analysis

XRD Analysis

Carbon steel coupons were immersing in 1M HCl for 48 hrs in absence and presence of optimum concentration of the inhibitors. The surface film composition was determined using X-ray powder diffractometer, PANalytical X, PERT PRO MPD (Netherland), with $\text{Cu K}\alpha$ radiation at a rating of 40 kV, 40 mA. The diffraction patterns were recorded at room temperature in the angular range of $40\text{--}80^\circ$ (2θ) with step size 0.02° (2θ) and scan step time 0.4 (s). The crystalline phases formed on the carbon steel surface were identifying using the ICDD-PDF database.

EDXA Analysis

The surface film developed on the metal specimen examined by energy dispersive X-ray analysis (EDXA), which carried out with an energy dispersive spectrometer in conjugation with a Jeol 5400 scanning electron microscope. The spectra recorded on samples immersed for a period of 48 hrs in 1.0M HCl in the absence and presence of optimum concentration of the inhibitor. The energy of the acceleration beam employed was 30 KV.

RESULTS AND DISCUSSION

Inhibitors Characterization

The author (Nassar *et al.*, 2011) characterized the synthesized compounds and their purity confirmed by thin layer chromatography (TLC). The X-Ray diffraction patterns for CdS shown in Fig. 1.

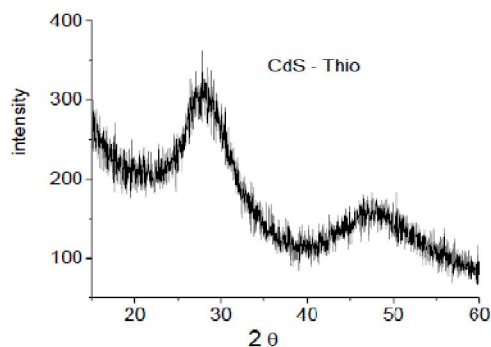


Fig. 1. XRD Pattern for CdS nanoparticles obtained in presence of thiophenol as a capping agent

The pattern shows peak at $2\theta = 28.10$, corresponding to hexagonal reflection (101) and scanned peak at $2\theta = 47.91$, corresponding to hexagonal state (103). This gives us indication that our product has a hexagonal structure. The crystallite size of CdS nanoparticles calculated from Scherer equation:

$$D = \frac{0.9\lambda}{\beta\cos\theta} \quad (1)$$

Where D = diameter of particles, λ = wavelength of XRD, θ = is the angle of diffraction, β = is the full- width at half-maximum (FMWH) of the peak. It was found that D = 2.7 nm for the prepared CdS.

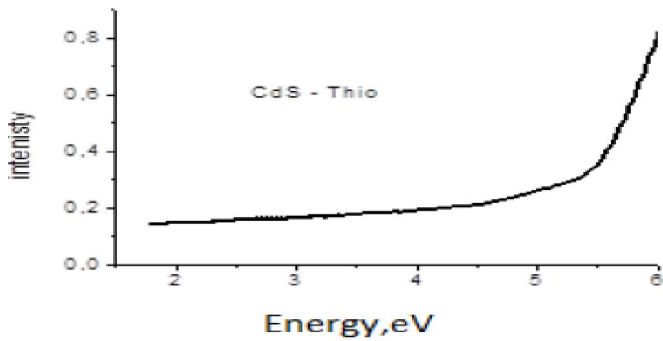


Fig. 2. Energy band gap for CdS nanoparticles obtained in presence of thiophenol as a capping agent

Fig. 2 displays the UV-vis absorption spectra of sized thiophenol-modified CdS (S-CdS; the surface ligands on the CdS nanoparticles are thiophenol units). The sharp absorption peak at $k = 5.13$ eV, arises from CdS nanoparticles with diameter of 2.7 nm as calculated from the following equation (Ravindran *et al.*, 1999)

$$E = 2.42 + \frac{2.42}{R^2} - \frac{0.3031}{R} \quad (2)$$

Where E= energy band gap for the prepared CdS; R = radius nanoparticles. The UV- spectra of CdS dispersed in PMMA shown in Fig. 3.

By comparing the data shown in Fig.2&3, it can be easily noticed that the value of E CdS (Energy band gap) for CdS in nanocomposite is lower than ECdS for pure CdS. Consequently, the size of CdS in nanocomposite is higher than that of CdS in the pure form. Scanning Electron Microscopy (SEM) confirmed this result as shown in Fig.4, the micrograph of CdS dispersed PMMA indicates the agglomeration of CdS nanoparticles up to 10 nm which still have good characteristics for our study.

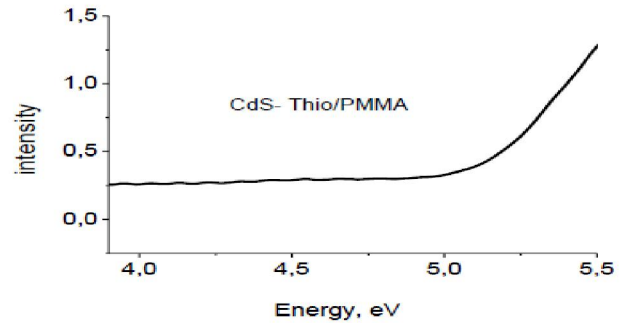


Fig. 3. Energy band gap for CdS nanoparticles and dispersed in PMMA

Weight Loss Measurements

Effect of Inhibitor Concentration

The values of percentage inhibition efficiency and corrosion rate obtained from weight loss measurements in 1.0 M HCl in presence of different concentrations of CdS and CdS\PMMA at various temperatures are reported in Tables 1 & 2 respectively. The inhibition efficiency ($\eta_w\%$) and surface coverage was determined by following equations (Bentiss and Lagrenne 2005):

$$\eta_w \% = \frac{W_o - W_i}{W_o} \times 100 \quad (3)$$

Table 1. Corrosion parameters for carbon steel in aqueous solution of 1 M HCl in absence and presence of different concentrations of CdS inhibitor from weight loss measurements at different temperatures for 6 h.

Temp.	1M HCl	CdS											
		1x10 ⁻⁴			5 x10 ⁻⁴			10 x10 ⁻⁴			15 x10 ⁻⁴		
	CR (mgcm ⁻² h ⁻¹)	CR (mgcm ⁻² h ⁻¹)	θ	η_w %	CR (mgcm ⁻² h ⁻¹)	θ	η_w %	CR (mgcm ⁻² h ⁻¹)	θ	η_w %	CR (mgcm ⁻² h ⁻¹)	θ	η_w %
298	2.003	1.383	0.31	31	0.783	0.61	61	0.611	0.69	69.5	0.541	0.73	73
303	2.532	1.899	0.25	25	1.139	0.55	55	0.886	0.65	65	0.785	0.69	69
313	3.080	2.433	0.21	21	1.546	0.498	49.8	1.223	0.60	60.3	1.108	0.64	64
323	3.692	3.064	0.17	17	2.049	0.445	44.5	1.624	0.56	56	1.476	0.60	60
333	4.747	4.082	0.14	14	2.706	0.43	43	2.278	0.52	52	2.041	0.57	57

Table 2. Corrosion parameters for carbon steel in aqueous solution of 1 M HCl in absence and presence of different concentrations of CdS\PMMA inhibitors from weight loss measurements at different temperature for 6 h.

Temp.	1M HCl	CdS/PMMA											
		1x10 ⁻⁴			5 x10 ⁻⁴			10 x10 ⁻⁴			15 x10 ⁻⁴		
	CR (mgcm ⁻² h ⁻¹)	CR (mgcm ⁻² h ⁻¹)	θ	η_w %	CR (mgcm ⁻² h ⁻¹)	θ	η_w %	CR (mgcm ⁻² h ⁻¹)	θ	η_w %	CR (mgcm ⁻² h ⁻¹)	θ	η_w %
298	2.003	0.95	0.526	52.6	0.341	0.83	83	0.261	0.87	87	0.200	0.90	90
303	2.532	1.519	0.40	40	0.684	0.73	73	0.456	0.82	82	0.357	0.859	85.9
313	3.080	2.196	0.287	28.7	1.093	0.65	64.5	0.708	0.77	77	0.573	0.814	81.4
323	3.692	2.769	0.25	25	1.495	0.60	60	1.037	0.72	72	0.853	0.769	76.9
333	4.747	3.77	0.205	20.5	2.22	0.53	53.3	1.56	0.67	67	1.29	0.729	72.9

Where W_i and W_o are the weight loss values in the presence and absence of inhibitor, respectively.

The corrosion rate (CR) of carbon steel was calculated as ($\text{mgcm}^{-2}\text{h}^{-1}$) using the relation:

$$\text{CR} = \frac{W}{St} \quad (4)$$

Where W is the average weight loss of carbon steel sheets, S is the total area of the specimen, and t is the immersion time. The variation of inhibition efficiency with the studied inhibitors concentration is shown in Fig. 5(a, b). It is noticed clearly that, both studied inhibitors inhibit the corrosion of carbon steel in HCl solution and the inhibition efficiency increases with the increase in concentration. This result is due to the fact that the adsorption amount and the degree of inhibitor coverage on carbon steel surface increases with increasing inhibitor concentration.

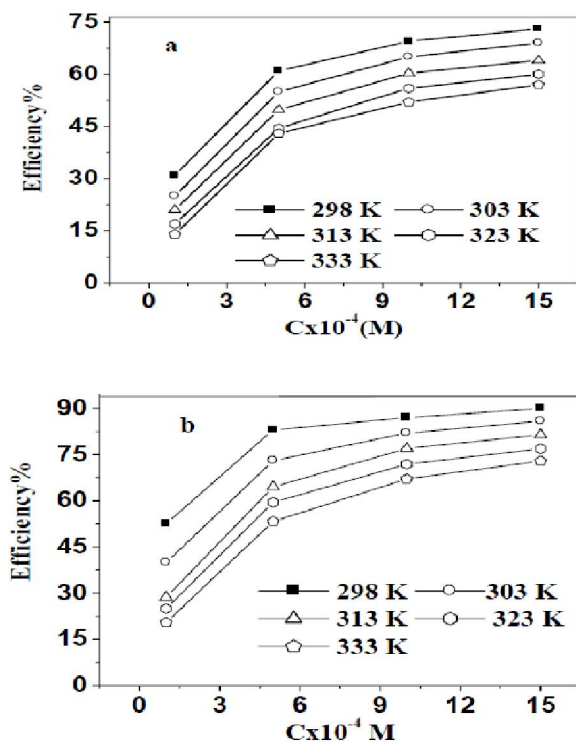


Fig. 5. Variation of inhibition efficiency of different concentrations of (a) CdS (b) CdS/PMMA on carbon steel in 1 M HCl

Effect of Temperatures

Temperatures effect on the corrosion rate studied in the temperature range 298–333 K using weight loss experiments. Results showed in Fig. 6 (a, b). As the temperature increases, the rate of corrosion increases and hence the inhibition efficiency of the inhibitors decreases. However, this decrease in $\eta\%$ is small at higher inhibitor concentration. This result can be attributed to the fact that desorption is aided by increasing the temperature. This behavior indicates that the adsorption of inhibitors on C-steel surface occurs through physical adsorption (Solomon *et al.*, 2010; Schorr and Yahalom 1972).

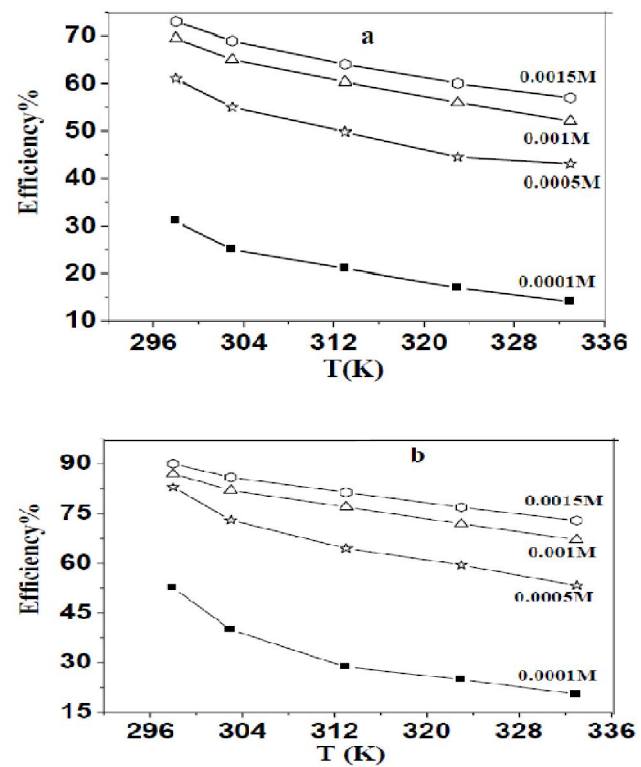


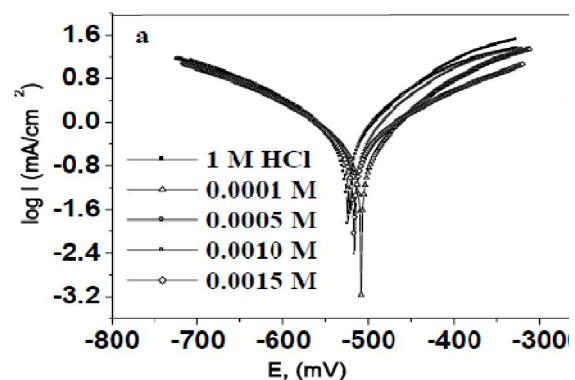
Fig. 6. Variation of inhibition efficiency of (a) CdS (b) CdS/PMMA on carbon steel in 1 M HCl at different temperatures

Electrochemical measurements

Potentiodynamic polarization measurements

Polarization measurements carried out in order to gain knowledge concerning the kinetics of the cathodic and anodic reactions. Fig. 7(a&b) presents the results of the effect of CdS and CdS/PMMA concentration on the cathodic and anodic polarization curves of carbon steel in 1 M HCl, respectively. From the polarization curves, it is clear that addition of CdS and CdS/PMMA to acid solutions shifts the anodic curves to more positive potentials and the cathodic curves to more negative potentials i.e. both anodic metal dissolution and cathodic hydrogen evolution reaction were inhibited.

This may be ascribed to the fact that, being adsorbed on the metal surface, CdS and CdS/PMMA controlled the anodic and cathodic reactions during corrosion process, and then its corrosion inhibition efficiency is directly proportional to the amount of adsorbed inhibitor.



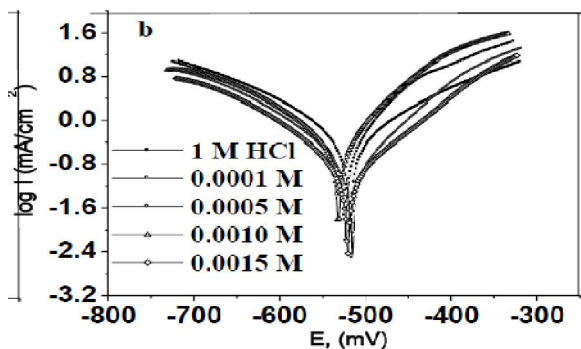


Fig. 7. Tafel Polarization of carbon steel in 1 M hydrochloric acid with different concentrations of (a) CdS (b) CdS/PMMA

The functional groups and structure of the inhibitor play important roles during the adsorption process (Prabhu *et al.*, 2008). Electrochemical corrosion kinetics parameters, i.e., corrosion potential (E_{corr}), cathodic and anodic Tafel slopes (β_a , β_c) and corrosion current density (I_{corr}) obtained from the extrapolation of the polarization curves, and calculated $\eta_i\%$ are listed in Tables (3&4). The corrosion inhibition efficiency ($\eta_i\%$) and surface coverage evaluated from the measured I_{corr} values using the relationships (Sahin *et al.*, 2002):

$$\eta_i \% = \frac{I_{corr}^0 - I_{corr}^1}{I_{corr}^2} \times 100 \quad (5)$$

where I_{0corr} and I_{1corr} are the corrosion current densities in the absence and in the presence of inhibitor, respectively.

As reflected from Tables 3&4 it is evident that the corrosion current density (I_{corr}) decreases upon the addition of CdS and CdS/PMMA inhibitors to HCl solution. Furthermore value of E_{corr} are not altered significantly and the maximum displacement was 9 and 12 mV for CdS and Cd/PMMA respectively, indicating the mixed type behaviour of the studied inhibitors (Ferreira *et al.*, 2004; Li *et al.*, 2008). Values of the inhibition efficiency were calculated and listed in Table (3&4), The data obtained reveal that the inhibition efficiency (η_i) increases as the inhibitor concentration increases and the order of inhibition efficiency increases as follows:

Table 3. The polarization parameters for CdS compound

Conc.	E_{corr} (mV)	i_{corr} mA/cm ²	R_p ohm.cm ²	β_a mV/dec	β_c mV/dec	θ	$\eta_i\%$
Blank	-517	1.19	53	202	-199	-	-
0.0001	-514	0.74	82	105	-145	0.378	37.8
0.0005	-522	0.46	87	80	-104	0.614	61.4
0.001	-522	0.38	95	82	-102	0.681	68.1
0.0015	-508	0.35	114	84	-108	0.706	70.6

Table 4. The polarization parameters for CdS/PMMA hybride compound

Conc.	E_{corr} (mV)	i_{corr} mA/cm ²	R_p ohm.cm ²	β_a mV/dec	β_c mV/dec	θ	$\eta_i\%$
Blank	-517	1.19	53	202	-199	-	-
0.0001	-529	0.45	60.3	59.3	-97	0.622	62.2
0.0005	-521	0.25	84	80.2	-96	0.789	78.9
0.001	-513	0.17	120	90.5	-92	0.857	85.7
0.0015	-519	0.13	158	90	-117	0.893	89.3

CdS < CdS/PMMA. Table 3 & 4 also show that, the studied inhibitor reduced both anodic and cathodic currents.

Electrochemical impedance spectroscopy

Impedance method provides information about the kinetics of the electrode processes and simultaneously about the surface properties of the investigated systems. The shape of impedance gives mechanistic information. The method is widely used for investigation of the corrosion inhibition processes (Hermas *et al.*, 2004). Electrochemical impedance measurements were carried over the frequency range from 100 kHz to 50 mHz at open circuit potential. The Nyquist representations of impedance behaviour of carbon steel in 1 M HCl with and without addition of various concentrations of CdS and CdS/PMMA given in Fig. 8(a&b) respectively. The measurements made after the stabilization of the electrode at OCP for one hour at room temperature. The figures show that the diameter of the semicircle increases with the increase in inhibitor concentration in the electrolyte, indicating an increase in corrosion resistance of the material. Impedance spectra obtained at each concentration of CdS and CdS/PMMA fitted to the electrical equivalent circuit presented in Fig. 9. The equivalent circuit consists of the double-layer capacitance (Cdl) in parallel to the charge transfer resistance (Rct), which was used previously to model the iron/acid interface and similar circuit have been described in the literature for the acidic corrosion inhibition of steel (Elayyachy *et al.*, 2006; Lece *et al.*, 2008). The charge transfer resistance values (Rct) were calculated from the difference between impedance values at the lower and higher frequencies as suggested by Haruyama *et al.* (1978). One constant phase element (CPE) is substituted for the capacitive element to give a more accurate fit, as the obtained capacitive loop is a depressed semi-circle. The depression in Nyquist semicircles is a feature for solid electrodes and often referred to as frequency dispersion and attributed to the roughness and other inhomogenities of the solid electrode (Mahadavian and Attar 2006). The CPE is a special element whose admittance value is a function of the angular frequency (ω), and whose phase is independent of the frequency. The relation (Singh *et al.*, 2011) gives the admittance and impedance of CPE;

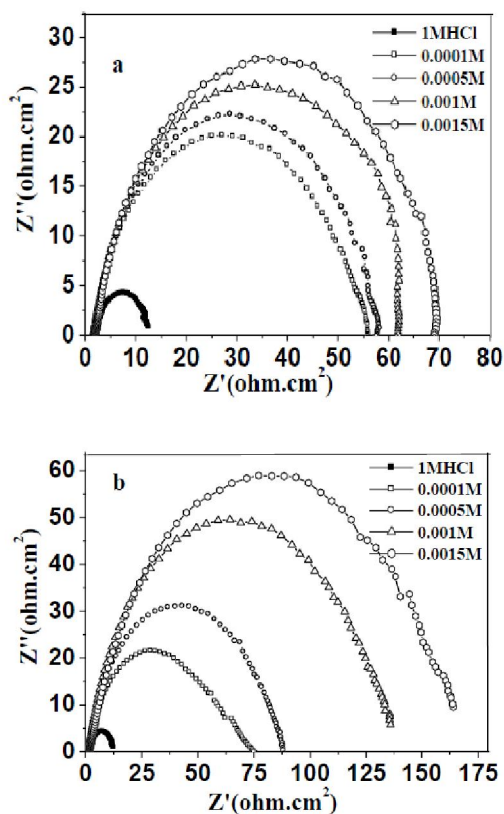


Fig.8. Nyquist plots for carbon steel in 1 M HCl in absence and presence of different concentrations of (a) CdS compound (b) CdS/PMMA compound

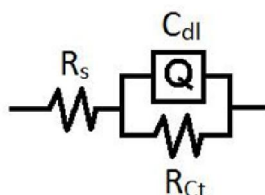


Fig.9. The electrochemical equivalent circuit used to fit the impedance measurements

$$Y_{CDE} = Y_0(i\omega)^{-n} \quad (6)$$

where, Y_0 is the magnitude of CPE, i is an imaginary number ($i^2 = -1$), n is the phase angle of CPE

and
$$n = \alpha/(\pi/2) \quad (7)$$

in which α is the phase angle of CPE.

The electrochemical parameters, Including R_s , R_{ct} , Y_0 and n , obtained from fitting the recorded EIS, using the electrochemical circuit, are listed in Table 5. In addition, the C_{dl} values derived from CPE parameters according to Eq. (7) (Singh *et al.*, 2011) are listed in Table 5.

$$C_{dt} = Y_0(\omega_{max})^{n-1} \quad (8)$$

where, ω_{max} is angular frequency $\omega_{max} = 2\pi f_{max}$ at which the imaginary part of impedance ($-Z_i$) is maximal and f_{max} is AC frequency at maximum. The inhibition efficiency percentage (η_z %) of corrosion of carbon steel is calculated from R_{ct} as follows (Hegazy 2009):

$$\eta_z = 1 - \frac{R_{ct}^0}{R_{ct}} \times 100 \quad (9)$$

where R_{ct}^0 and R_{ct} are charge transfer resistance values with and without inhibitors, respectively.

The charge transfer resistance (R_{ct}) increases consequently, the double layer capacitance (C_{dl}) decreases as the concentration of the inhibitors increases. Indicating the decreased of the corrosion rate and the increased corrosion inhibition, this may be due to the increase in the surface coverage by the inhibitor leading to an increase in the inhibition efficiency that attributed to the adsorption of the inhibitor at the metal surface causing a change in the double layer structure. The decrease in C_{dl} , which results from local dielectric constant decrease and/or an increase in the thickness of the electrical double layer, suggests that these molecules act by adsorption on the metal/solution interface (Muralidharan *et al.*, 1995). Hence, changes in R_{ct} and C_{dl} values caused by the gradual replacement of the water molecules by adsorption of inhibitor on carbon steel surface, reducing the extent of dissolution (Trachli *et al.*, 2002). Polarization measurements and EIS study are in good agreement with each other.

Adsorption isotherm

Adsorption depends mainly on the charge and nature of the metal surface, electronic characteristics of the metal surface, adsorption of solvent and other ionic species, temperature of corrosion reaction and on the electrochemical potential at solution interface (Trabanelli 1987). Adsorption isotherms usually used to describe the adsorption process. The establishment of adsorption isotherms that describe the adsorption of a corrosion inhibitor can provide important clues to the nature of the metal-inhibitor interaction (Abd El-Rehim *et al.*, 1999; Khamis 2004). Adsorption of the organic molecules occurs as the interaction energy between molecule and metal surface is higher than that between the H_2O molecule and the metal surface (Moretti *et al.*, 1994). In order to obtain the adsorption isotherm, the degrees of surface coverage (θ) for various concentrations of the inhibitor have calculated according to Eq. (2). Langmuir isotherm tested for its fit to the experimental data. Langmuir isotherm given by following

Table 5. The calculated parameters obtained from equivalent circuit fitting analysis with and without inhibitors in HCl

Inhibitor	Conc. of inhibitor	$R_s \Omega.cm^2$	n	$R_{ct} \Omega.cm^2$	$C_{dl} \mu F.cm^{-2}$	η_{ct}
Blank	1M HCl	2.39	0.88	10.77	186	-
CdS	0.0001M	1.79	0.86	53	105	79.67
	0.0005M	1.79	0.87	54	84	80
	0.0010M	2.12	0.87	61	67	82
	0.0015M	1.83	0.86	67	76	85
	0.0001M	1.71	0.85	70	65	84.6
CdS/PMMA	0.0005M	1.56	0.86	87	56	87.6
	0.0010M	1.86	0.80	135	47	92
	0.0015M	1.77	0.82	164	43	93.4

equation (Hegazy and Zaky 2010; Zhao and Mu 1999; Mu *et al.*, 2006; Abiola and Otaigbe 2009; Oguzie *et al.*, 2004):

$$\frac{C}{\theta} = \frac{1}{K_{ads}} + C_{inhb} \quad (10)$$

where, K_{ads} is the equilibrium constant of the adsorption-desorption process, θ is the degree of surface coverage and C is molar concentration of inhibitor in the bulk solution.

Fig. 10 shows the relationship between C/θ and C for the prepared CdS and CdS/PMMA and the linear regressions and the slopes of C/θ and C plot were calculated and listed in Table 6&7. It is clear that, all the linear correlation coefficients (R^2) are almost equal to 1 and all the slopes are very close to 1, which indicates that, the adsorption of inhibitors onto carbon steel surface obeys the Langmuir adsorption isotherm (Langmuir 1947).

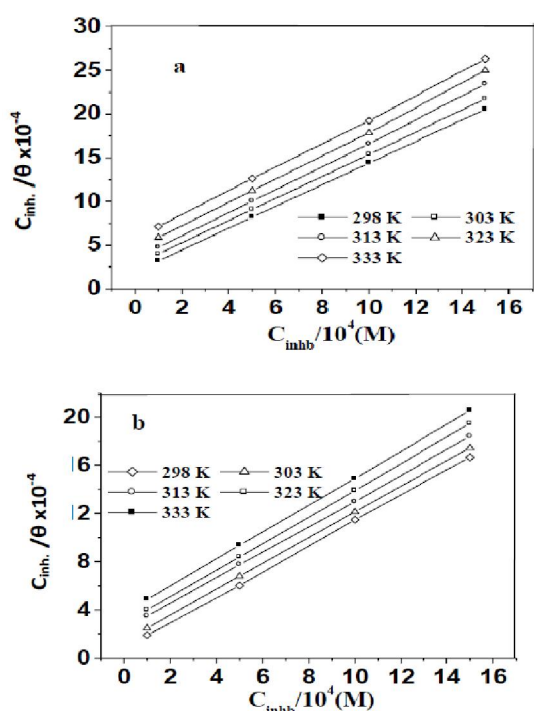


Fig.10. Langmuir isotherms for adsorption of the (a) CdS and (b) CdS/PMMA on the CS surface in 1 M HCl

The equilibrium constant for the adsorption process from Langmuir related to the standard free energy of adsorption by the expression (Schorr 1972):

$$K_{ads} = \frac{1}{55.5 \exp(-\Delta G_{ads}^0/RT)} \quad (11)$$

where, R is the molar gas constant, T is the absolute temperature and 55.5 is the concentration of water in solution expressed in molar. The standard free energy of adsorption ΔG_{ads}^0 , can characterize the interaction of adsorption molecules and metal surface, calculated by Equ. 9; Generally, values of ΔG_{ads}^0 up to -20 kJ mol $^{-1}$ consistent with the electrostatic interaction between the charged molecules and the charged metal (physical adsorption) while those more negative than -40 kJ mol $^{-1}$ involve sharing or transfer of electrons from the inhibitor molecules to the metal surface to form a coordinate bond (chemisorptions) (Bentiss *et al.*, 2009; Ali *et al.*, 2008; Saliyan and Adhikari 2008). As seen from Tables 6&7, the values of ΔG_{ads}^0 decrease as temperature increases and more negative than -20 kJ mol $^{-1}$. The negative values of ΔG_{ads}^0 , indicate the spontaneous and probably of chemical and physical adsorption for inhibitor in 1.0 M HCl. The adsorption is enhanced by the presence of Cd atoms with lone pairs of electrons and S atoms in the inhibitor molecules that make it able to be adsorbed electrostatically on the metal surface forming insoluble stable films on the metal surface thus decreasing metal dissolution. The adsorption heat (ΔH_{ads}^0) can be calculated according to the Van't Hoff equation (Haruyama *et al.*, 1978):

$$\ln K_{ads} = -\Delta H_{ads}^0/RT + \text{constant}$$

When $\ln K_{ads}$ vs. $(1/T)$ plotted, the values of (ΔH_{ads}^0) obtained from the slope and, (ΔS_{ads}) obtained for a range of temperatures with the following equation (Mu *et al.*, 2004).

$$\Delta G_{ads}^0 = \Delta H_{ads}^0 - T\Delta S_{ads} \quad (12)$$

It noted that $\Delta H_{ads}^0/R$ is the slope of the straight line $\ln K_{ads} - 1/T$ according to Eq. (11) and the molecular weight of inhibitor a positive constant, so the value of adsorption heat does not change with the unit of adsorptive equilibrium constant. The straight line $\ln K_{ads} - 1/T$ showed in Fig. 11. Because that it is close to standard to standard condition, the adsorption heat under such experimental conditions (Li *et al.*, 2008).

Table 6. Standard thermodynamic parameters of adsorption on carbon steel surface in 1 M HCl containing different concentrations of the prepared CdS

Temperatures, (K)	K_{ads} , (mol $^{-1}$)	Slope	R^2	ΔG_{ads}^0 (kJmol $^{-1}$)	ΔH_{ads}^0 (kJmol $^{-1}$)	ΔS_{ads}^0 (Jmol $^{-1}$)
298	5028	1.2	1	-31	-22.1	104
303	3648	1.3	1	-30.9		102
313	2953	1.3	0.999	-31.25		100
323	2252	1.3	0.999	-31.52		98
333	1737	1.3	0.999	-31.77		95

Table 7. Standard thermodynamic parameters of adsorption on carbon steel surface in 1 M HCl containing different concentrations of the prepared CdS/PMMA

Temperatures, (K)	K_{ads} , (mol $^{-1}$)	Slope	R^2	ΔG_{ads}^0 (kJmol $^{-1}$)	ΔH_{ads}^0 (kJmol $^{-1}$)	ΔS_{ads}^0 (Jmol $^{-1}$)
298	12287	1.09	0.999	-33.4	-19.704	112
303	6873	1.1	0.998	-32.43		107
313	4141	1.2	0.999	-32.13		103
323	3473	1.2	0.998	-32.7		101
333	2662	1.3	0.998	-32.95		99

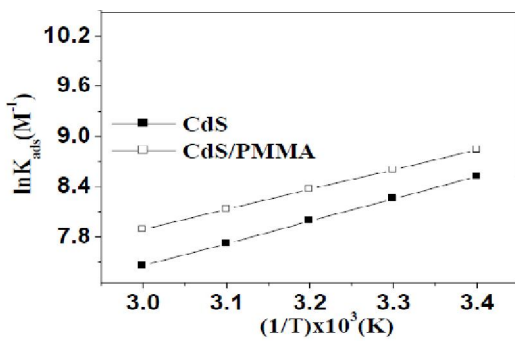


Fig.11. The relationship between $\ln K_{ads}$ and $(1/T)$ of the CdS and CdS/PMMA in 1 M HCl at various temperatures

The negative values of show that, the adsorption of the ΔH_{ads}^0 inhibitors is an exothermic process that indicates that the inhibition efficiency decreases with the temperature increasing. As the values of heat of adsorption for the inhibitor is less than -40 kJ mol^{-1} , the physical adsorption mechanism suggested (Gomma and Wahdan 1995; Jha 1990).

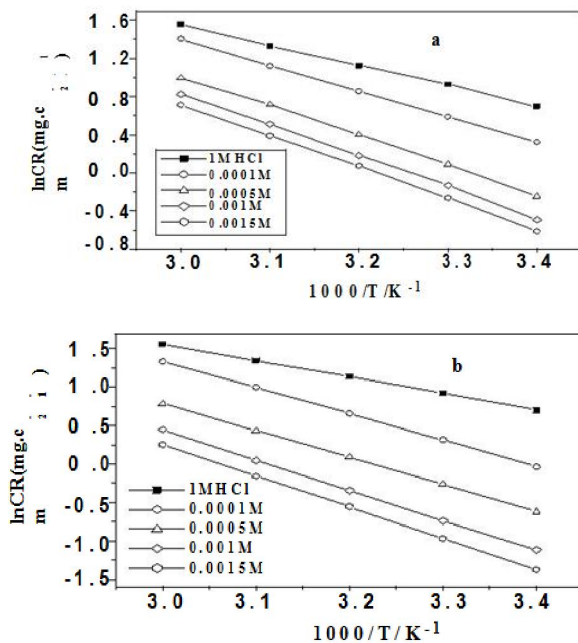


Fig. 12. Adsorption isotherm plots of $\ln(CR)$ vs. $1000/T/K^{-1}$ in absence and presence of different concentrations of (a) CdS and (b) CdS/PMMA at various temperatures

Thermodynamic parameters

It has been reported by number of authors (Elachouri *et al.*, 1996; Mu *et al.*, 2004; Qiu *et al.*, 2008) that in acid solution of carbon steel, logarithm of the corrosion rate is a linear function with $1/T$ (Arrhenius equation); (Quraishi and Khan 2005; Breslin and Carrol 1993; Khedr and Lashien 1992): $\ln CR = -E_a^0/RT + \ln A$ (14) where, E_a^0 is the apparent effective activation energy, R general gas constant and A the Arrhenius pre exponential factor. A plot of \ln of corrosion rate, obtained by weight loss measurement, vs $1/T$ gave straight line as shown in Fig. 12 (a & b). The values of activation energy E_a^0 obtained from the slope of the lines are given in Table 8. The value of E_a^0 of solution containing CdS and CdS.PMMA is higher than that of free acid solution, indicating the physical adsorption (Larabi *et al.*, 2007). An alternative formula of the

Arrhenius equation is the transition state equation (Abd El Rehim *et al.*, 2001):

$$CR = \frac{RT}{N h_{exp} \Delta S_a^0} \exp\left(\frac{\Delta H_a^0}{RT}\right) \quad (15)$$

where h is Plank's constant, N the Avogadro's number, ΔS_a^0 the entropy of activation and ΔH_a^0 the enthalpy of activation. A plot of $\ln(CR/T)$ vs $1/T$ gave a straight line (Fig. 13 a&b), with a slope of $(\Delta H_a^0/R)$ and an intercept of $(\ln RT/Nh + \Delta S_a^0/R)$, from which the values of Table 8. The positive sign of enthalpy reflect the endothermic that dissolution of steel is difficult ΔS_a^0 and ΔH_a^0 were calculated and listed in nature of steel dissolution process meaning

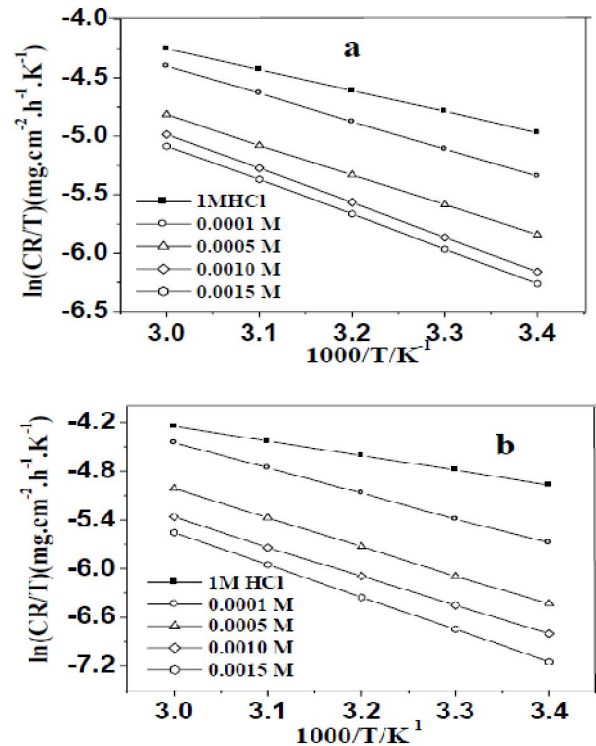


Fig. 13. Adsorption isotherm plots of $\ln(CR/T)$ vs. $1000/T/K^{-1}$ in absence and presence of different concentrations of (a) CdS and (b) CdS/PMMA at various temperatures

On comparing the values of entropy of activation listed in Table 8, it is clear that entropy of activation increased in presence of the studied inhibitor compared to free acid solution. Such variation is associated with the phenomenon of ordering and disordering of inhibitor molecules on the mild steel surface. The increased entropy of activation in the presence of inhibitor indicates that disorderness is increased on going from reactant to activated complex.

Surface film Analysis

X-Ray Diffraction analysis

The X-ray diffraction patterns of the film formed on the carbon steel surface immersed in 1 M HCl in the absence and presence of CdS and CdS/ PMMA are shown in Fig. 14 (a, b and c) respectively. Identification of the phases formed on the surface in the absence of inhibitor (Fig. 14 a) revealed the formation of oxide layer composed of $FeOOH$ (goethite) and Fe_3O_4 (magnetite). This result is typical for carbon steel in environments that contain chloride (Gil *et al.*, 2003).

Table 8. Standard thermodynamic parameters of adsorption on carbon steel surface in 1 M HCl containing different concentrations of the prepared CdS and CdS/PMMA

compound	Inhibitor Conc./Mx 10 ⁻⁴	ΔE_a^\ddagger (kJ mol ⁻¹)	ΔG_a^\ddagger (kJ mol ⁻¹)	ΔH_a^\ddagger (kJ mol ⁻¹)	ΔS_a^\ddagger (J mol ⁻¹)
Blank	1M HCl	18	56	-14	-189
CdS	1	22	61	-20	-202
	5	26	65	-23	-208
	10	27	68	-24	-211
	15	28	70	-24	-211
CdS/PMMA	1	28	67	26	-220
	5	29	71	30	-227
	10	32	73	30	-225
	15	34	80	35	-240

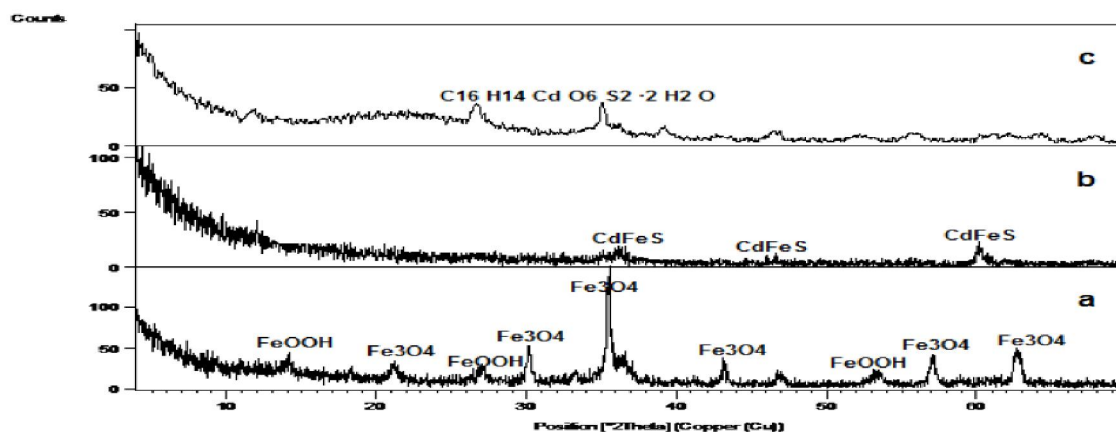


Fig.14. XRD patterns of the film formed on the surface of carbon steel after 48 h of immersion in (a) 1M HCl; (b) 1 M HCl+ CdS ; (c) 1 M HCl + CdS/PMMA at 25°C ±

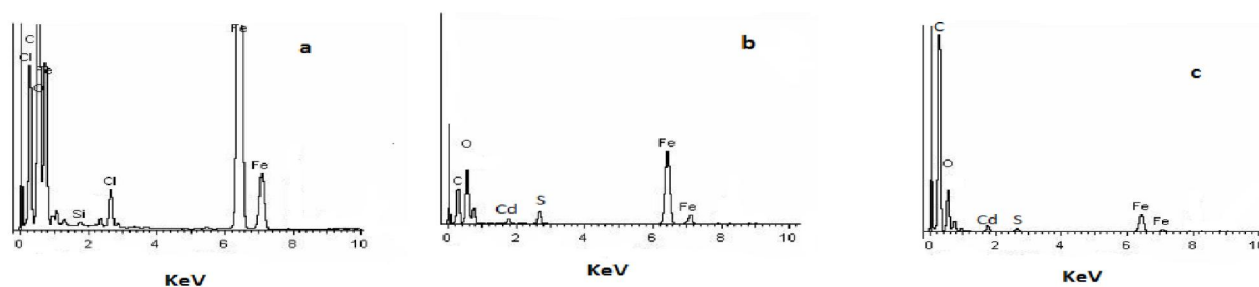


Fig. 15. EDX spectra of carbon steel specimens, After 48 h of immersion in (a) 1.0 M HCl ; (b) 1.0 M HCl + CdS and (c) 1.0 M HCl + CdS/PMMA

The XRD pattern of the film formed in presence of CdS as an inhibitor (Fig. 14 b) shows a relative smooth pattern with some characteristic peaks of CdFeS. This is expected to be the adsorbed film on carbon steel surface responsible for corrosion inhibition. The enhancement of corrosion inhibition of carbon steel upon hybridizing CdS with PMMA is explained via the identification of phase compositions of the film formed on CdS/ PMMA inhibited surface, which indicates the formation of organic layer of C₁₆ H₁₄ Cd O₆ S₂ · 2H₂O as shown in (Fig.14 c). This layer acts as a barrier and provides protection to carbon steel surface against acidic dissolution.

Energy Dispersive X-ray analysis

EDX technique employed in order to determine which elements were present on carbon steel surface before and after the exposure to the inhibitors solutions. After carbon, steel coupons immersed in 1 M HCl solution in the absence and

presence of optimum concentration of CdS, CdS/PMMA for 48 h, and its surface film composition was determined by EDX, and the results are displayed in Fig. (15).

EDX panorama recorded for carbon steel without inhibitor treatment (Fig. 15a) shows iron and carbon signals, which are the characteristics peaks of the main elements constituting the carbon steel sample. Also, some peaks characterizing oxygen and chloride are detected; these peaks represent the corrosion products formed on the surface (chloride and oxide). In presence of CdS, as inhibitor, the spectrum (Fig. 15b) shows Cd and S signals also, it can be easily noticed that the Fe peaks are considerably suppressed relative to the samples immersed in 1 M HCl, free of inhibitor; the Cl and O peaks are also suppressed. The suppression of the Fe, Cl and O lines can be attributed to the overlying inhibitor film over the carbon steel sample indicating that, the corrosion inhibition process was

related to the development of an inhibitor film over the metal surface. In presence of Cd/PMMA (Fig. 15c), the EDX spectra did not show additional lines. However, the carbon and oxygen signals significantly enhanced upon adding Cd /PMMA to HCl solutions. This enhancement in carbon and oxygen signals is due to the carbon and oxygen atoms of the adsorbed Cd /PMMA species. These data show that a carbonaceous material containing oxygen atoms has covered the electrode surface. This layer is undoubtedly due to the inhibitor, because of the high contribution of the carbon and oxygen signals observed in presence of Cd /PMMA. This high contribution is not present on the electrode surface exposed to uninhibited HCl solutions (Fig. 15a). Thus, (EDX) observations of the electrode surface confirmed the existence of an adsorbed film over the surface.

Conclusion

1. CdS acts as efficient corrosion inhibitor for carbon steel in HCl solution and CdS/PMMA shows enhanced inhibition efficiency.
2. The inhibition efficiency increases the increasing the inhibitors concentration but decreases with the temperature increase.
3. The polarization measurements reveal that CdS and CdS/PMMA behave as mixed-type inhibitors in 0.1 M HCl by acting on both anodic metal dissolution and cathodic hydrogen evolution reactions.
4. The adsorption of the inhibitors on the surface of CS in 0.1 M HCl follows a Langmuir adsorption isotherm. The high value of adsorption equilibrium constant and the negative value of standard free energy of adsorption suggested that is CdS/PMMA is strongly adsorbed on CS surface.
5. EDX analysis and XRD examinations of the surface film confirmed the existence of such adsorbed film.

REFERENCES

- Abd El Rehim S. S., Hassan H. H., Amin M. A., 2001. Corrosion inhibition of aluminum by 1,1(lauryl amido)propyl ammonium chloride in HCl solution. *Mater. Chem. Phys.* 70, 1, 64–72.
- Abd El-Rehim S. S., Magdy A., Ibrahim M., Khaled F., 1999. 4-Aminoantipyrine as an inhibitor of mild steel corrosion in HCl solution. *J. Appl. Electrochem.* 29, 5, 593–599.
- Abiola O. K., Otaigbe J. O. E., 2009. The effects of *Phyllanthus amarus* extract on corrosion and kinetics of corrosion process of aluminum in alkaline solution. *Corros. Sci.* 51, 11, 2790 - 2793.
- Ali S. A., Al-Muallem H. A., Saeed M.T., Rahman S.U., 2008. Hydrophobic-tailed bicycloisoxazolidines: A comparative study of the newly synthesized compounds on the inhibition of mild steel corrosion in hydrochloric and sulfuric acid media. *Corros. Sci.* 50, 3, 664 - 675.
- Ameer M. A., Khamis E., Al-Motlaq M., 2004. Electrochemical behaviour of recasting Ni–Cr and Co–Cr non-precious dental alloys. *Corros. Sci.* 46, 11, 2825–2836.
- Bardel E., 2003. Corrosion and Protection, Springer-Verlag, London,
- Bentiss F., Lagrenne M., 2005. Thermodynamic characterization of metal dissolution and inhibitor adsorption processes in mild steel/2,5-bis(n-thienyl)-1,3,4-thiadiazoles/hydrochloric acid system. *Corros. Sci.* 47, 12, 2915- 2931.
- Bentiss F., Lebrini M., Vezin H., Chai F., Traisnel M., Lagrené M., 2009. Enhanced corrosion resistance of carbon steel in normal sulfuric acid medium by some macrocyclic polyether compounds containing a 1,3,4-thiadiazole moiety: AC impedance and computational studies. *Corros. Sci.* 51, 9, 2165 - 2173.
- Breslin C. B., Carrol W. M., 1993. The activation of aluminium by indium ions in chloride, bromide and iodide solutions. *Corros. Sci.* 34, 2, 327–341.
- Brinker C. J., Scherer G. W., 1990. Sol–gel science, Academic Press: The Physics and Chemistry of Sol-Gel Processing, San Diego, 787, 839–880.
- Chazeau L., Cavaille J. Y., Canova G. R., Dendievel R., Boutherein B., 1999. Viscoelastic properties of plasticized PVC reinforced with cellulose whiskers. *J. Appl. Polym. Sci.* 71, 11, 1797-1808.
- Elachouri M., Hajji M. S., Salem M., Kertit S., Aride J., Coudert R., Essassi E., 1996. Some Nonionic Surfactants as Inhibitors of the Corrosion of Iron in Acid Chloride Solutions. *Corrosion* 52, 2, 103 - 108.
- Elayyachy M., El Idrissi A., Hammouti B., 2006. New thio-compounds as corrosion inhibitor for steel in 1 M HCl. *Corros. Sci.* 48, 9, 2470 -2479.
- Favier V., Canova G. R., Shrivastava S. C., Cavaille J. Y., 1997. Mechanical percolation in cellulose whisker nanocomposites. *Polym. Eng. Sci.* 37, 10, 1732 – 1739.
- Feil F., Fu"rbeth W., Schu"tze M., 2008. Nanoparticle based inorganic coatings for corrosion protection of magnesium alloys. *Surface Engineering* 24, 198-203.
- Ferreira E. S., Giancomelli C., Giacomelli F. C., Spinelli A., 2004. Evaluation of the inhibitor effect of l-ascorbic acid on the corrosion of mild steel. *Mater. Chem. Phys.* 83, 1, 129–134.
- Gil M. L. A., Santos A., Bethencourt M., Garcia T., ernández-Bastero S., Velo A., Gago- Dupor L., 2003. Use of X-ray and other techniques to analyses the phase transformation induced in archaeological cast iron after its stabilisation by the electrolytic method. *Chemical Acta.* 494, 1-2, 245-254.
- Gomma M. K., Wahdan M. H., 1995. Schiff bases as corrosion inhibitors for aluminium in hydrochloric acid solution. *Mater. Chem. Phys.* 39, 3, 209 - 213.
- Haruyama S., Tsuru T., Gijutsu B., 1978. Corrosion inhibition of iron by amphoteric surfactants in 2M HCl. *J. Jpn.Soc. Corros. Eng.* 27, 573 -581.
- Hegazy M. A., 2009. A novel Schiff base-based cationic gemini surfactants: Synthesis and effect on corrosion inhibition of carbon steel in hydrochloric acid solution. *Corros. Sci.* 51, 11, 2610- 2618.
- Hegazy M. A., Zaky M. F., 2010. Inhibition effect of novel nonionic surfactants on the corrosion of carbon steel in acidic medium. *Corros. Sci.* 52, 4, 1333 –1341.
- Hegazy, M. A., Badawi A. M., Abd El Rehim S. S., Kamel W. M., 2013. Corrosion inhibition of carbon steel using novel N-(2-(2-mercaptoacetoxy) ethyl)-N, N-dimethyl dodecan-1-aminium bromide during acid pickling. *Corros. Sci.*, 69, 110 –122.
- Hermas A. A., Morad M. S., Wahdan M. H., 2004. Effect of PgTPhPBr on the electrochemical and corrosion behaviour

- of 304 stainless steel in H₂SO₄ solution. *J. Appl. Electrochem.* 34, 1, 95–102.
- Jha J. L., 1990. Studies of the Adsorption of Amide Derivative During Acid Corrosion of Pure Iron and its Characterization, Ph.D. Thesis, Delhi University, Delhi.
- Khedr M.G. A., Lashien M.S., 1992. The role of metal cations in the corrosion and corrosion inhibition of aluminium in aqueous solutions. *Corros. Sci.* 33, 1, 137–151.
- Larabi L., Benali O., Harek Y., 2007. Corrosion inhibition of cold rolled steel in 1 M HClO₄ solutions by N-naphtyl N'-phenylthiourea. *Mater. Lett.* 61, 14-15, 3287 - 3291.
- Lece H. D., Emregul K. C., Atakol O., 2008. Difference in the inhibitive effect of some Schiff base compounds containing oxygen, nitrogen and sulfur donors. *Corros. Sci.* 50, 5, 1460 - 1468.
- Li W. H., He Q., Pei C. L., Hou B. R., 2008. Some new triazole derivatives as inhibitors for mild steel corrosion in acidic medium. *J. Appl. Electrochem.* 38, 3, 289–295.
- Li X., Deng S., Mu G., Fu H., Yang F., 2008. Inhibition effect of nonionic surfactant on the corrosion of cold rolled steel in hydrochloric acid. *Corros. Sci.* 50, 2, 420 - 430.
- Liu J. D. M., 1998. Densification of Zirconia from Submicron-Sized To Nano-Sized Powder Particles. *Mater. Sci. Lett.* 17, 467–469.
- Mahadavian M., Attar M. M., 2006. Another approach in analysis of paint coatings with EIS measurement: Phase angle at high frequencies. *Corros. Sci.* 48, 12, 4152–4157.
- Moretti G., Quartarone G., Tassan A., Zingales A., 1994. Inhibition of mild steel corrosion in 1N sulphuric acid through indole. *Mater. Corros.* 45, 12, 641–647.
- Mu G. N., Li X. H., Qu Q., Zhou J., 2006. Molybdate and tungstate as corrosion inhibitors for cold rolling steel in hydrochloric acid solution. *Corros. Sci.* 48, 2, 445 - 459.
- Mu G. N., Li X. M., Li F., 2004. Synergistic inhibition between o-phenanthroline and chloride ion on cold rolled steel corrosion in phosphoric acid. *Mater. Chem. Phys.* 86, 1, 59 - 68.
- Muralidharan S., Phani K. L. N., Pitchumani S., Ravichandran S., 1995. Polyamino - Benzoquinone Polymers: A New Class of Corrosion Inhibitors for Mild Steel. *J. Electrochem. Soc.*, 142, 5, 1478 - 1483.
- Nassar I. M., Osipova V. V., Safiullin G., Lobkov V., Galyametdinov Yu., 2011. Preparation of II-VI semiconductors nanoparticles and investigation of their photophysical properties. *International. J. of Green Nanotechn.* 3, 1, 22-36.
- Oddo, J. E., Tomson M. B., 1982. Simplified Calculation of CaCO₃ Saturation at High Temperatures and Pressures in Brine Solutions. *J. Pet. Tech.* 34, 1583 - 1590.
- Oguzie E. E., Unaegbu C., Ogukwe C. N., Okolue B. N., Onuchukwu A. I., 2004. Inhibition of mild steel corrosion in sulphuric acid using indigo dye and synergistic halide additives. *Mater. Chem. Phys.* 84, 2-3, 363–368.
- Popova A., Christor M., Raicheva S., Sokolova E., 2004. Adsorption and inhibitive properties of benzimidazole derivatives in acid mild steel corrosion. *Corros. Sci.* 46, 6, 1333 -1350.
- Prabhu R. A., Venkatesha T. V., Shanbhag A. V., Kulkarni G. M., Kalkhambkar R. G., 2008. Inhibition effects of some Schiff's bases on the corrosion of mild steel in hydrochloric acid solution. *Corros. Sci.* 50, 12, 3356 -3362.
- Qiu L. G., Wu Y., Wang Y. M., Jiang X., 2008. Synergistic effect between cationic gemini surfactant and chloride ion for the corrosion inhibition of steel in sulphuric acid. *Corros. Sci.* 50, 2, 576 - 582.
- Quraishi M. A., Khan S., 2005. Thiadiazoles-A potential class of heterocyclic inhibitors for prevention of mild steel corrosion in hydrochloric acid solution. *Indian J. Chem. Technol.* 12, 576–581.
- Ravindran T. R., Akhilesh K. A., Balamurugan B., Mehta B. R., 1999. Inhomogeneous broadening in the photoluminescence spectrum of CdS nanoparticles. *J. Nanostructure Materials.* 11, 5, 603 – 609.
- Ridd, B., T. J. Blakset, D. Queen, 1998. Corrosion, NACE, 78, Houston, Texas.
- Sahin M., Blgic S., Yilmaz H., 2002. The inhibition effects of some cyclic nitrogen compounds on the corrosion of the steel in NaCl mediums. *Appl. Surf. Sci.* 195, 1-4, 1–7.
- Saliyan V. R., Adhikari A.V., 2008. Quinolin-5-ylmethylene-3-[[8-(trifluoromethyl)quinolin-4-yl]thio}propanohydrazide as an effective inhibitor of mild steel corrosion in HCl solution. *Corros. Sci.* 50, 1, 55 - 61.
- Schorr M., Yahalom J., 1972. The significance of the energy of activation for the dissolution reaction of metal in acids. *Corros. Sci.* 12, 11, 867-87.
- Schorr M., Yahalom J., 1972. The significance of the energy of activation for the dissolution reaction of metal in acids. *Corros. Sci.* 12, 11, 867–868.
- Shikha T., Sanjay T., 2006. Electrical and optical properties of CdS nanocrystalline semiconductors. *Cryst. Res. Technol.* 41, 1, 78-82.
- Singh A. K., S. K. Shukla, M. Singh, M.A. Quraishi, 2011. Inhibitive effect of ceftazidime on corrosion of mild steel in hydrochloric acid solution. *Mater. Chem. Phys.* 129, 1-2, 68–76.
- Solomon M. M., Umoren S. A., Udosoro I. I., Udoh A. P., 2010. Inhibitive and adsorption behaviour of carboxymethyl cellulose on mild steel corrosion in sulphuric acid solution. *Corrosion Science*, 52, 4, 1317–1325.
- Tang L. B., Mu G. N., Liu G. H., 2003. The effect of neutral red on the corrosion inhibition of cold rolled steel in 1.0 M hydrochloric acid. *Corros. Sci.* 45, 10, 2251-2262.
- Trabanelli G., 1987. Chemical Industries: Corrosion Mechanism F. Mansfeld (Ed.), New York, Marcel Dekker, 120.
- Trachli B., Keddami M., Takenouti H., Srhiri A., 2002. Protective effect of electropolymerized 3-amino 1, 2, 4-triazole towards corrosion of copper in 0.5 M NaCl. *Corros. Sci.*, 44, 5, 997 - 1008.
- Varela Caselis J. L., Rubio Rosas E., Castan˜o Meneses V. M., 2012. Hybrid PMMA–silica anticorrosive coatings for stainless steel 316Lg. *Corros. Eng. Sci. and Tech.* 47, 2, 131-137.
- Wolfrom M. L., Thompson A., 1947. Derivatives of N-Methyl-L-glucosaminic Acid; N-Methyl-L-mannosaminic Acid. *J. Am. Chem. Soc.* 69, 8, 1847 - 1849.
- Zhao T. P., Mu G. N., 1999. The adsorption and corrosion inhibition of anion surfactants on aluminium surface in hydrochloric acid. *Corros. Sci.* 41, 10, 1937 - 1944.
- Zheludkevich M. L., Miranda Salvado I., Ferreira M. G. S., 2005. Sol–gel coatings for corrosion protection of metals. *J. Mater. Chem.* 15, 5099–5111.